Queensland University of Technology
Brisbane Australia

This is the author's version of a work that was submitted/accepted for publication in the following source:

Lin, Tian Ran, Tan, Andy C. C., Ma, Lin, & Mathew, Joseph (2011) Estimating the loading condition of a diesel engine using instantaneous angular speed analysis. In Lee, Jay (Ed.) *Proceedings of the 6th World Congress on Engineering Asset Management*, Springer, Duke Energy Center, Cincinnati, Ohio. (In Press)

This file was downloaded from: http://eprints.qut.edu.au/46609/

© Copyright 2011 Please consult the authors

Notice: *Changes introduced as a result of publishing processes such as copy-editing and formatting may not be reflected in this document. For a definitive version of this work, please refer to the published source:*

Proceedings of the 6th World Congress on Engineering Asset Management
Cincinatti, Ohio, USA
3-5 October, 2011

ESTIMATING THE LOADING CONDITION OF A DIESEL ENGINE USING INSTANTANEOUS ANGULAR SPEED ANALYSIS

Tian Ran Lin [a, b], Andy C. C. Tan [b], Lin Ma [a, b] and Joseph Mathew [a]

[a] CRC for Infrastructure and Engineering Asset Management, Brisbane QLD 4001 Australia

[b] School of Engineering Systems, Queensland University of Technology, Brisbane QLD 4001 Australia

Abstract: Continuing monitoring of diesel engine performance is critical for early detection of fault developments in the engine before they materialize and become a functional failure. Instantaneous crank angular speed (IAS) analysis is one of a few non intrusive condition monitoring techniques that can be utilized for such tasks. In this experimental study, IAS analysis was employed to estimate the loading condition of a 4-stroke 4-cylinder diesel engine in a laboratory condition. It was shown that IAS analysis can provide useful information about engine speed variation caused by the changing piston momentum and crankshaft acceleration during the engine combustion process. It was also found that the major order component of the IAS spectrum directly associated with the engine firing frequency (at twice the mean shaft revolution speed) can be utilized to estimate the engine loading condition regardless of whether the engine is operating at normal running conditions or in a simulated faulty injector case. The amplitude of this order component follows a clear exponential curve as the loading condition changes. A mathematical relationship was established for the estimation of the engine power output based on the amplitude of the major order component of the measured IAS spectrum.

Keywords: Condition monitoring, Diesel engine performance, Instantaneous angular speed, Order analysis

1. INTRODUCTION

Diesel engines are one of the most critical classes of machinery in industry today. Unpredicted failures of diesel engines can cause dire consequences. It is thus essential to mitigate unpredicted engine failures to ensure continuing operation and optimum engine performance. Engine failures could be caused either by combustion related subsystems, such as the fuel injection system, the cylinder/piston system, the inlet and outlet valve system, or by non-combustion related subsystems including all auxiliary devices such as turbochargers, gears, bearings and electronic control units. Faults developed in combustion related subsystems will directly affect the combustion process and engine performance. Engine misfire, knocking, insufficient power output, poor fuel efficiency, excessive exhaust smoke, excessive noise and vibration are some of the most typical fault symptoms of a diesel engine. To minimize or to prevent the occurrence of unpredicted engine failures, the operating state and health of a diesel engine needs to be monitored continually so that a fault symptom and its cause could be diagnosed and dealt with at the early stage before it becomes a functional failure.

Instantaneous crank angular speed and in-cylinder pressure methods are two commonly employed condition monitoring techniques for engine performance monitoring and combustion related fault detections. In-cylinder pressure technique can provide a direct indication of engine performance and the state of the engine combustion process. However, applications of the technique are restrained by the intrusive nature of the method. Furthermore, in-cylinder pressure measurement is a localized technique which can only detect or monitor the combustion process of the cylinder where a pressure sensor is mounted. Prompted by the rapid development of data acquisition hardware and signal processing techniques over the last decade or two, a non intrusive instantaneous angular speed (IAS) measurement is gaining wide applications for condition monitoring and fault detection of rotating machinery. For instance, IAS technique was successfully employed for torsional vibration analysis [1, 2], condition monitoring of gear transmission [2-5], condition monitoring and fault detection of diesel engines [6-9], condition monitoring of electric motors [10] and roller bearing fault detection [11]. Instantaneous angular speed (IAS) technique can also be employed for monitoring engine performance as the variation of crank angular speed is directly correlated to the total gas pressure torque produced by the engine combustion process.

In the application of IAS for fault detection and diagnosis of diesel engines, Yang et al [6] presented a simple two-degree of freedom dynamic system for the simulation of instantaneous angular speed fluctuation of a four-stroke four-cylinder diesel engine. They found that the instantaneous angular speed is largely affected by the tangential force induced by the gas pressure and the vertical imbalance inertial force induced by piston acceleration/deceleration of all the cylinders. They further illustrated that the fluctuation of IAS can be utilized for detecting engine combustion related faults such as those affecting the gas pressure in the cylinders, i.e., fuel or exhaust valve leakages. Charles et al [7] extended the IAS technique further for condition monitoring and fault diagnosis of large diesel engines with a high number of cylinders. By presenting the IAS waveform in a polar coordinate system, they demonstrated that IAS waveform can be utilized to detect and identify the faulty (misfiring) cylinder of two relatively large multicylinder diesel engines (16 and 20 cylinders respectively). Taraza et al [8] investigated the amplitude change of order components of IAS waveforms of two diesel engines and correlated the amplitude of the lowest major harmonic order (order 2 for a 4-cylinder engine and order 3 for a six-cylinder engine) of IAS spectra to that of the gas pressure torque produced by the engine combustion. They also illustrated that phases of the three lowest order components of the IAS spectrum could be utilized to identify the faulty cylinder of a diesel engine. Douglas et al [9] applied both acoustic emission and instantaneous angular speed techniques for on-line power estimation of two large marine diesel engines. They found that the calculated standard deviation of IAS waveforms in each engine cycle changes accordingly to the loading condition of the two marine engines under test. The change patterns also agreed well with those of the measured acoustic emission (AE) root mean squared (RMS) energy per engine cycle at various loading conditions.

Recently, Li et al [12] presented a comprehensive discussion for optimizing IAS measurements and provided a detailed IAS error analysis. Gu et al [13] developed a theoretical model for noise reduction of IAS signals by employing a combined FFT and Hilbert transform. They then implemented the method to reduce the noise in IAS data acquisition and its influence on the IAS estimation and fault diagnosis of a rotor-shaft test rig.

The two most common approaches for instantaneous angular speed measurements are time/counter based method and analogue to digital conversion (ADC) based method [12]. ADC-based methods, which use only standard data acquisition equipment, are much easier to implement in practical situations than time/counter based methods. The principle of ADC based methods is to acquire analogue encoder signals from the rotating shaft where the encoder is attached onto and then converts the signal into digital data at a fixed sampling frequency. Thus, the IAS data can be extracted directly from raw encoder signals and the method is less likely to be affected by ambient noise. An ADC based IAS method is employed in this study for the diesel engine performance monitoring and is extended further for diesel engine fault detection which will be reported separately [14].

The contents presented in this paper are arranged as follows: Section 2 presents a description of the test rig and the experimental setup for data acquisition and condition monitoring of a diesel engine. An order analysis of IAS waveforms extracted from raw encoder signals are presented in Section 3. Discussion and insightful comments of the results obtained from this investigation are also offered in the section. Section 4 summarizes the main findings from this study.

2. THE DIESEL ENGINE TEST RIG AND EXPERIMENTS

Simulating common diesel engine faults in a controlled manner under laboratory conditions, and characterizing the signal patterns of simulated faults at various loading conditions can provide instantaneous and accurate fault diagnosis of diesel engines since faults in a diesel engine do not normally occur in a short period of time. To this end, a GEP18-4 Olympian diesel engine generator set as shown in Fig. 1(a) was used in the fault simulation and experimental investigation presented in this paper. The specification of the engine is described in Table 1. The diesel engine generates a nominal power output of about 15kW. A three-phase 15kW industrial fan heater as showed in Fig. 1(b) was used to absorb the power output generated by the diesel engine generator set in the experiment. The fan heater which has three heat settings was adjusted for various engine loadings during the experiment.

The sensors used in the simulation study included four resonance type (PAC Micro-30D) acoustic emission sensors, a (Kistler) high temperature pressure sensor and an (PCB) ICP piezoelectric accelerometer as shown in Fig. 1. A combined optical encoder and top dead centre (TDC) recording unit taken out from the electronic distributor of a Nissan Bluebird car was also installed onto the crankshaft next to the flywheel for the measurement of instantaneous angular speed and torsional vibration. The encoder has 360 circumferential evenly spaced slits (1^0 resolution) and it was assumed that the encoder was ideally manufactured with negligible manufacturing errors. The circumferential space between two sequential slits of the encoder is about the same as the span of each slit. The flywheel on the crankshaft reduced engine speed fluctuations, particularly at the unloaded conditions.

The other sensors installed on the diesel engine test rig were for comparative studies of their effectiveness in condition monitoring and fault detection under various simulated faults.

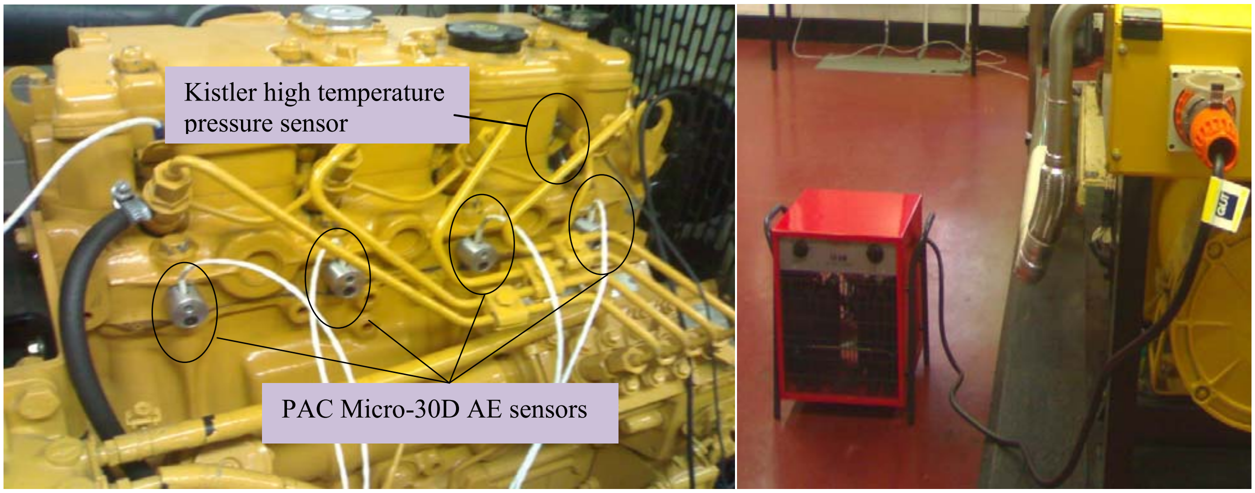

(a) (b)

Fig. 1 Graphical illustration of the diesel engine test rig and sensors; (a) the test rig, and (b) the industry fan heater.

A multi-channel National Instrument data acquisition card (DAQ Card-6062E) with a sampling frequency of up to 500kHz, coupled with a Labview software installed on a laptop computer were used for the data acquisition of encoder signals in the experiment. The sampling frequency in the measurement was set at 100kHz, which was pre-determined according to the following equation to minimize the IAS measurement errors [13]

$$f_s > 4[nf_{shaft} + (n_h f_{shaft} + n\Delta f)] \, , \tag{1}$$

where f_s is the sampling frequency, n is the number of circumferential evenly spaced slits of the encoder, n_h is the highest order of IAS components of concern, f_{shaft} is the shaft rotating frequency and Δf is the estimated shaft speed variation.

Table 1 Diesel Engine Specification

Perkins 404C-22 engine data	
Number of cylinders	4
Arrangement	In-line
Running speed	1500 rpm
Bore	84.0mm
Stroke	100.0mm
Displacement	2.216 litres
Compression ratio	23.3:1
Firing order	1-3-4-2
Injection timing (estimated)	15 degrees (+/- 1 degree) before TDC
Exhaust valve open (measured)	143 degrees after TDC
Exhaust valve close (measured)	370 degrees after TDC
Inlet valve open (measured)	354 degrees after TDC
Inlet valve close (measured)	584 degrees after TDC

The length of each data record was 5s which encompasses about 124~130 shaft revolutions in each data file depending on engine loading conditions. Ten (10) data files were recorded for each engine loading at the steady state condition. These data files were used for offline averaging in the order domain during the post processing of the IAS data to minimize the effect of amplitude variation on the signal characterization of the diesel engine.

3. INSTANTANEOUS ANGULAR SPEED ANALYSIS

The measured encoder signal (within a small time window) of the unloaded diesel engine at the normal running condition is shown in Fig. 2. The measured encoder signal was used to construct the instantaneous angular speed (IAS) waveform in the study. From the measured encoder signal, the instantaneous angular speed was calculated approximately by

$$\omega(t) = \frac{\partial \varphi(t)}{\partial t} \cong \frac{\varphi_j - \varphi_{j-1}}{\Delta t_j} \quad (\text{rad/s}), \tag{2}$$

where φ_j and φ_{j-1} are the crank angles of two sequential slits of the encoder, and Δt_j is the time difference between the two slits.

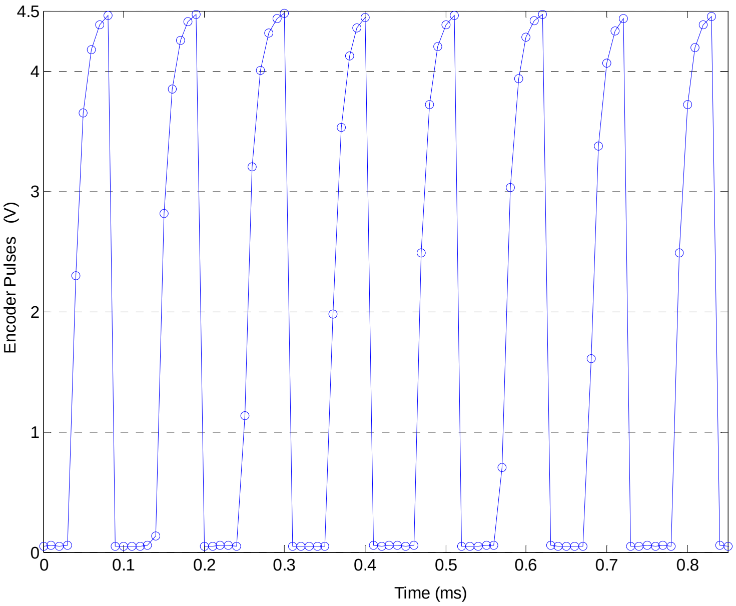

Fig. 2 Raw encoder signal at the engine unloaded condition

When examining the amplitude and the data point distribution of encoder pulses shown in Fig. 2, it was found that the distribution of data point locations of each encoder pulse was slightly different from each other. For a more accurate estimation of the instantaneous crank angular speed, a simple algorithm was implemented in the post processing of the encoder signal. In this implementation, the first data point on the rising edge of each encoder pulse which passes through a pre-defined amplitude threshold was identified first. A linear interpolation algorithm was then employed for a more accurate estimation of the time when a pulse passed the threshold value. An amplitude threshold value of 4V was chosen after examining the data point distribution in Fig. 2 to minimize the time estimation error in the linear interpolation algorithm. Procedures of the linear interpolation algorithm in processing the encoder signal will be described in detail separately [14].

3.1 IAS at normal engine running conditions

The IAS waveform of the diesel engine at the unloaded condition calculated using the linear interpolation algorithm [14] and Eq. (2) is shown in Fig. 3. The power spectrum of the IAS waveform displayed in the order domain is shown in Fig. 4. The major order components of the IAS spectrum can be correlated to major mechanical events of the diesel engine. For instance, the first major dominant order component of the IAS spectrum is attributed to the shaft rotating speed, the second order component corresponds to the engine firing frequency of the 4-stroke 4-cylinder diesel engine, while the fourth order component corresponds to the four top (bottom) dead centres of the diesel engine per shaft revolution. The identification of major order components of the IAS spectrum to the mechanical events of the diesel engine is not the objective of this work. Instead, the study aims to reveal and correlate the changing pattern of the major order component of the IAS spectrum to the power output (loading) of the diesel engine.

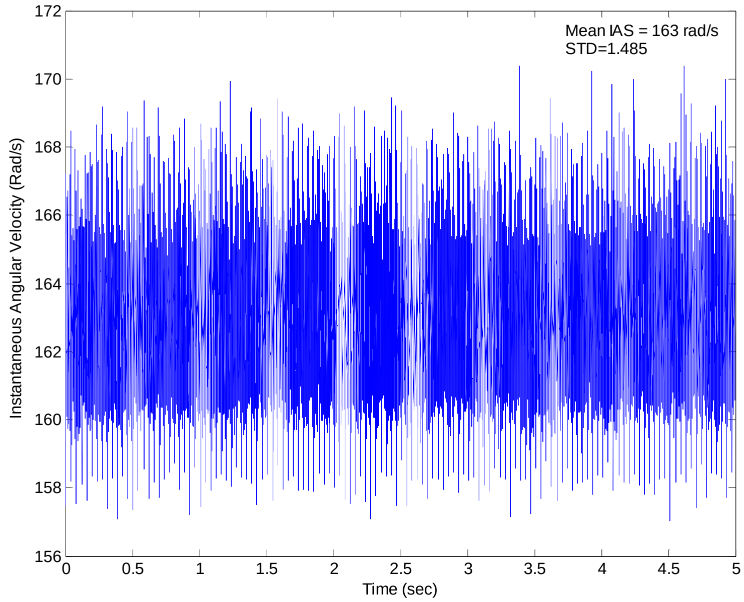

Fig. 3 Time waveform of the calculated instantaneous angular speed at an unloaded condition

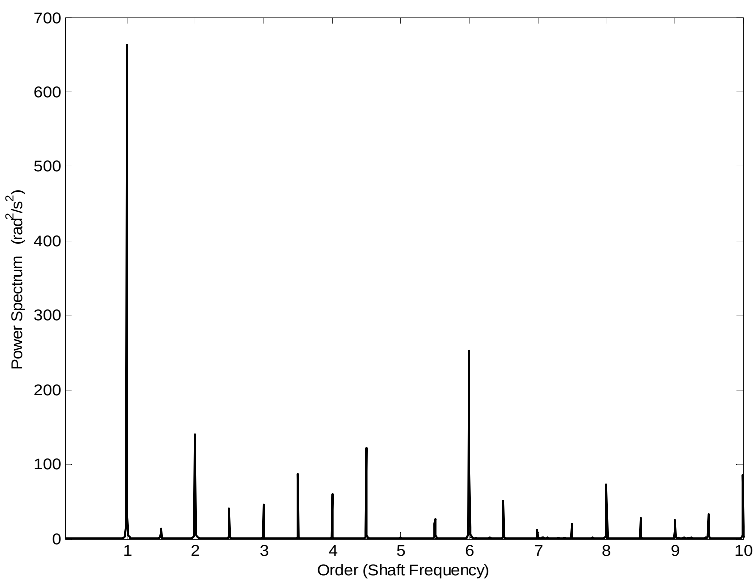

Fig. 4 Power Spectrum of the IAS waveform at an unload condition

3.2 Standard deviation per engine cycle of the IAS waveform at various loading conditions

Engine power output estimation was studied by Douglas et al [9] using an acoustic emission technique and standard deviation per engine cycle of IAS waveforms for two large marine diesel engines. In their work, they studied the change pattern of standard deviation per engine cycle of IAS waveforms at two loading conditions for one of the two test engines and three loading conditions for the other engine. They observed that the changing pattern of standard deviation per engine cycle of IAS waveforms is consistence with the changing power output of the diesel engine at the loading conditions under study. A major drawback of their work is that it did not provide a quantification analysis to establish an explicit mathematical relationship to describe the power output change by the amplitude change of the standard deviation.

In this study, the standard deviation per engine cycle of IAS waveforms of the diesel engine under four loading conditions, namely, unload, one third load, two third load and full load, is calculated according to [9]:

$$\sigma_i = \sqrt{\frac{1}{n-1}\sum_{j=1}^{n}(\omega_j - \bar{\omega}_i)} \, , \qquad (3)$$

where n is the length of the IAS data of the i^{th} engine cycle, ω_j is the IAS at the time instance t_j and $\bar{\omega}_i$ is the mean IAS for the i^{th} engine cycle.

The results are shown in Fig. 5. It is observed that the amplitude of the standard deviation per engine cycle of the IAS waveform decreases as the engine loading condition increases for the first three loading conditions. However, the trend does not continue for the last loading condition when the engine is running at full load. The result indicates that the standard deviation method may have limited applications in practical cases, for instance, to be used for engine loading estimation at low engine loading conditions. To overcome such limitation, an alternative method is developed in this study for diesel engine output power estimation, which is elaborated in the next section.

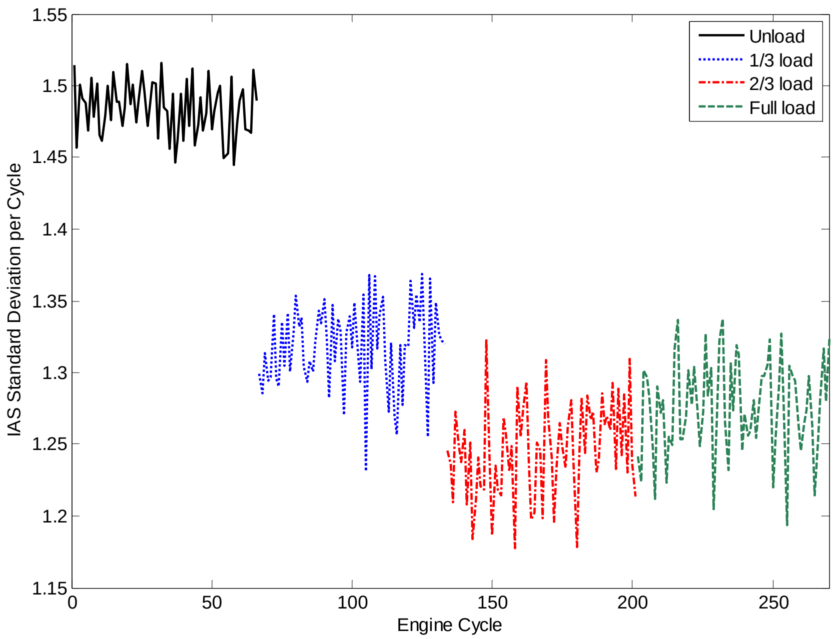

Fig. 5 Standard deviation per engine cycle of IAS signals at various engine loading conditions

3.3 Correlation between the major order component of an IAS spectrum and the engine loading condition

In this section, the correlation relationship between the amplitude of the major order component of the IAS spectrum and the loading condition of the diesel engine is established. The major order component of the IAS spectrum used in the study is the order component directly associated with the engine firing frequency. To minimize the effect of the engine speed and amplitude variation to the analysis, the IAS spectrum was averaged over the ten encoder files in the order domain for each engine loading condition, namely, unloaded (0kW), one-third load (5kW), two-third load (10kW) and full load (15kW). The major order component corresponding to the engine firing frequency (combustion) of the IAS spectrum at various loading conditions is shown in Fig. 6 for comparison. It is observed that the amplitude of the order component follows a clear exponential curve. This exponential curve can be described by the following equation

$$\mathbf{A} = A_0 \mathrm{e}^{(\alpha * \mathbf{N})}, \qquad (\mathrm{rad/s})^2, \qquad (4)$$

where **A** is the amplitude vector of the power spectrum component at various engine loading conditions, A_0 is the amplitude of the IAS power spectrum component at the unload condition, **N** is the vector indicating the loading conditions of the engine, which takes the value of 0 for unload condition and 1 for full load condition. $\mathbf{N} = \lfloor 0 \quad 1/3 \quad 2/3 \quad 1 \rfloor^T$ for the case presented in this study where T indicates a vector transpose.

The coefficient α in Eq. (4) can be determined by a least square curve fit as

$$\alpha = \frac{\mathbf{N}^T \ln(\frac{\mathbf{A}}{A_0})}{\mathbf{N}^T \mathbf{N}}, \tag{5}$$

where α =1.6873 was found for the case shown in Fig. 6.

Once the relationship between the engine loading condition and the amplitude of the order component is established and the amplitude of the order component at the unload condition is known, the power output of the diesel engine at any particular instance can be estimated by the amplitude (A_j) of the order component of the measured encoder signal at the instance as

$$N_j = \frac{1}{\alpha} \ln \frac{A_j}{A_0}, \tag{6}$$

where N_j is the normalized engine power output (with respect to the nominal engine output power) at the t_j time instance.

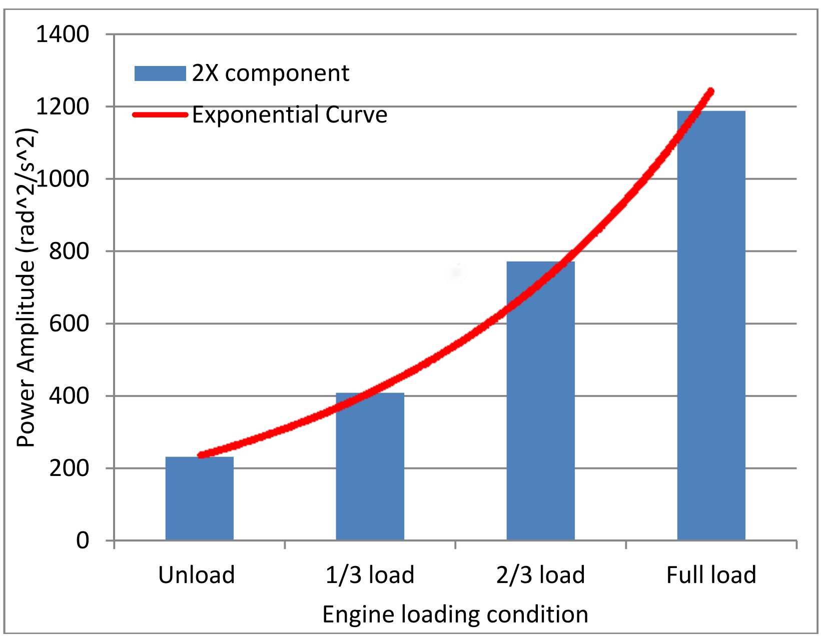

Fig. 6 Power amplitude of the order component corresponding to the engine firing frequency

The trend of amplitude change of this order component (correlates to the engine firing frequency) can be explained by the effect of changing engine loading condition on the engine combustion process and the gas pressure torque. Fig 7 shows the averaged in-cylinder pressure of cylinder 1 (the data was averaged over 180 engine cycles using a time waveform event driving synchronizing averaging technique in which the averaging process was correlated and triggered by the major mechanical events of the diesel engine to overcome the difficulty of averaging quasi-periodic signals in the time domain) at the four engine loading conditions. It is illustrated that the increase engine loading not only increased the peak amplitude of the engine combustion pressure (slightly) but also enlarged the area under the in-cylinder pressure curve. This indicates an increase gas pressure torque during the engine combustion when the loading increased, and thus led to the increased amplitude for the order component of the IAS spectrum correlating to the engine (combustion) firing frequency.

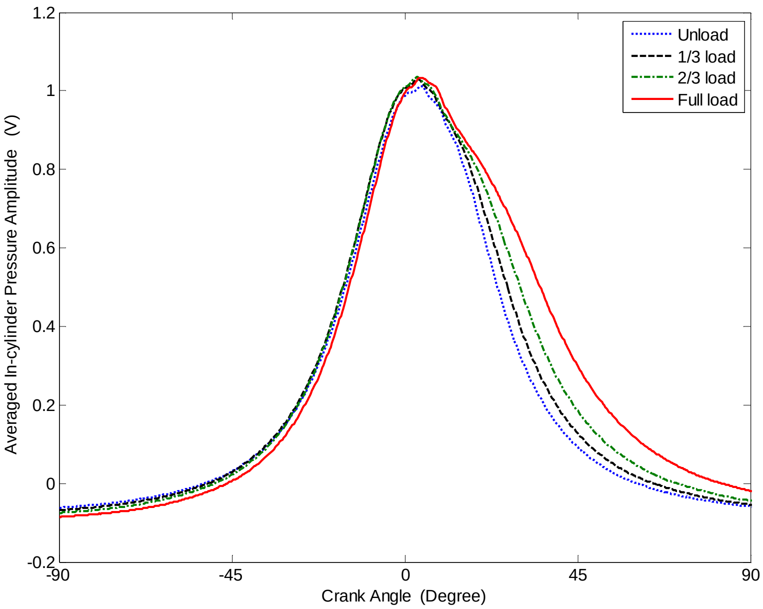

Fig. 7 Comparison of the averaged in-cylinder pressure of cylinder 1 at various loading conditions

3.4 The order component of the IAS spectrum at a simulated injector fault condition

To examine whether the pattern shown in Fig. 6 can also be found at other engine operating conditions such as engine running with a faulty injector, one was implanted into cylinder 1 of the engine test rig in the fault simulation experiment. The faulty injector is shown in Fig. 8 where a part of the pintle head of the injector was grounded off to simulate a defect of fuel spreading pattern during the fuel injection in the cylinder. It was found from the in-cylinder pressure measurement that the simulated injector fault (representing an incipient injector fault) had only a very small effect on the engine combustion pressure. It was also found that the IAS analysis at various engine loading conditions did not provide useful conclusive information for the detection of this simulated injector fault. This part of the analysis is not presented here to limit the scope of this paper. Examinations of amplitude change of the same order component of the IAS spectrum as showed in Fig. 9 revealed that the change in amplitude of the order component also followed an exponential curve in the simulated injector fault case. This curve can be described by an exponential relationship similar to Eq. (4) with a slightly modified coefficient α' and the unload base amplitude A'_0 as

$$\mathbf{A}' = A'_0 \mathrm{e}^{(\alpha' * \mathbf{N})}. \quad (7)$$

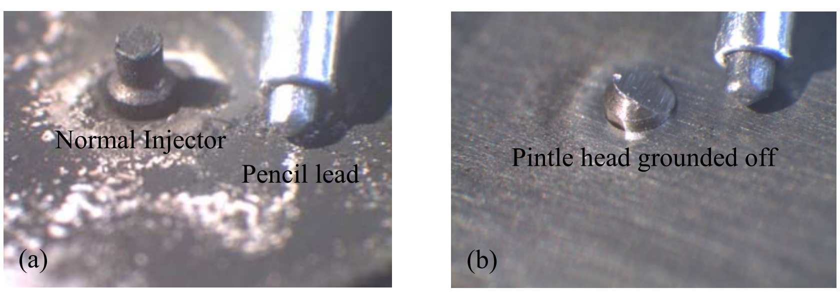

Fig. 8 The simulated injector fault; (a) normal injector head; (b) pintle head partly grounded off.

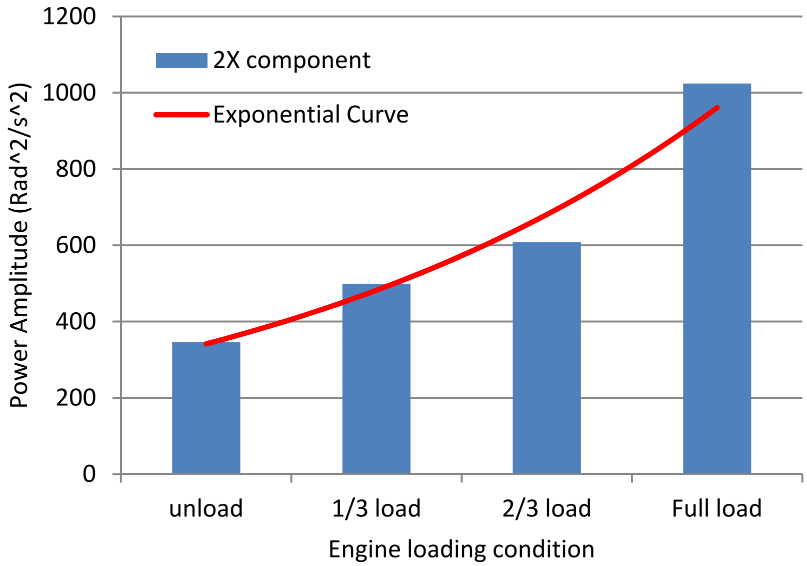

Fig.9 Power amplitude of the order component corresponding to the cylinder firing frequency at the faulty injector case

4. CONCLUSION

In this paper, an instantaneous angular speed analysis technique is presented for the estimation of engine power output and condition monitoring of diesel engines. It is shown that IAS analysis can provide useful information about engine speed variation caused by changing piston momentum and crankshaft acceleration and can also be used for engine power output estimation in both normal running and faulty injector conditions. It is found that the method of standard deviation per engine cycle of an IAS waveform [9] can only be employed to estimate the diesel engine power output at low loading conditions.

The low frequency order components of the IAS spectrum of a diesel engine can be traced back to major mechanical events of the diesel engine. In particular, it is found in this study that the changing amplitude of the order component of the IAS spectrum corresponding to the engine firing frequency follows a clear exponential curve to the changing engine loading condition. This trend can be explained by the fact that the amplitude of this order component is directly associated with the engine combustion process and the gas pressure torque whose amplitude also increases with increased engine loading conditions. A mathematical relationship was established in the study for the in-situ estimation of engine power output based on changing amplitude of the order component of the IAS spectrum corresponding to the engine firing frequency. The revelation of the correlation relationship between this order component and the engine loading condition as well as the mathematical model established in this work, can be employed for engine loading monitoring in practical applications.

ACKNOWLEDGEMENTS

This paper was developed within the CRC for Infrastructure and Engineering Asset Management, established and supported under the Australian Government's Cooperative Research Centres Programme. The authors gratefully acknowledge the financial support provided by the CRC.

REFERENCES

1. M. Feldman and S. Seibold, *Damage diagnosis of rotors: application of Hilbert transform and multihypothesis testing.* Journal of Vibration and Control (1999) **5**: pp 421-442.
2. D. Remond, *Practical performances of high-speed measurement of gear transmission error or torsional vibrations with optical encoders.* Measurement Science and Technology (1998) **9**: pp 347-353.

3. C. J. Stander and P. S. Heyns, *Instantaneous angular speed monitoring of gearboxes under non-cyclic stationary load conditions.* Mechanical Systems and Signal Processing (2005) **19**(4): pp 817-835.
4. S. Du and R. B. Randall, *Encoder error analysis in gear transmission error measurement.* Proceedings of the Institution of Mechanical Engineers, Part C: Journal of Mechanical Engineering Science (1998) **212**: pp 277-285.
5. P. J. Sweeney and R. B. Randall, *Gear transmission error measurement using phase demodulation* Proceedings of the Institution of Mechanical Engineers, Part C: Journal of Mechanical Engineering Science (1996) **210**(3): pp 201-213.
6. J. YANG, L. Pu, Z. Wang, Y. Zhou and X. Yan, *Fault detection in a diesel engine by analysing the instantaneous angular speed.* Mechanical Systems and Signal Processing (2001) **15**(3): pp 549-564.
7. P. Charles, J. K. Sinha, F. Gu, L. Lidstone and A. D. Ball, *Detecting the crankshaft torsional vibration of diesel engines for combustion related diagnosis.* Journal of Sound and Vibration (2009) **321**: pp 1171-1185.
8. D. Taraza, N. A. Henein and W. Bryzik, *The frequency analysis of the crankshaft's speed variation: a reliable tool for diesel engine diagnosis.* Transactions of the ASME, Journal of engineering for gas turbines and power (2001) **123**: pp 428-432.
9. R. M. Douglas, J. A. Steel, R. L. Reuben and T. L. Fog, *On-line power estimation of large diesel engine using acoustic emission and instantaneous crankshaft angular velocity.* Proceedings of the Institutions of Mechanical Engineers, International Journal of Engine Research (2006) **7**: pp 399-410.
10. A. Y. B. Sasi, F. Gu, B. Payne, A. Ball, *Instantaneous angular speed monitoring of electric motors.* Journal of Quality in Maintenance Engineering (2004) **10**(2): pp 123-135.
11. L. Renaudin, F. Bonnardot, O. Musy, J. B. Doray and D. Remond, *Natural roller bearing fault detection by angular measurement of true instantaneous angular speed.* Measurement Science and Technology (2010) **24**: pp 1998-2011.
12. Y. Li, F. Gu, G. Harris, A. Ball, N. Bennett and K. Travis, *The measurement of instantaneous angular speed.* Mechanical Systems and Signal Processing (2005) **19**: pp 786-805.
13. F. Gu, I. Yesilyurt, Y. Li, G. Harris and A. Ball, *An investigation of the effects of measurement noise in the use of instantaneous angular speed for machine diagnosis.* Mechanical Systems and Signal Processing (2006) **20**: pp 1444-1460.
14. T. R. Lin, A. C. C. Tan, L. Ma and J. Mathew, *Condition monitoring and fault diagnosis of diesel engines using instantaneous angular speed analysis.* Mechanical Systems and Signal Processing (2011) (In preparation).